American Journal of Physical Chemistry
2026, Vol. 15, No. 1, pp. 8–21
https://doi.org/10.11648/j.ajpc.20261501.12

Research Article

Isotherm, Kinetic and Thermodynamic Modelling of Biosorption of Methlyene Blue and Rhodamine 6G Dyes into Melon (*Cucumeropsis Manni)* Husk from Model Wastewater

Onwordi Chionyedua Theresa[1], Adetunji Ibrahim Olaniyi[1], Borokinni Ridwan Aderenle[1], Oyewole Toyib Seun[1], Uche Cosmos Chinedu[1], Osifeko Olawale Lawrence[1], Tovide Oluwakemi Omotunde[1], Osundiya Medinat Olubunmi[1], Dodo Salimah Wuraola[1], Akoro Seide Modupe[2], Olowu Rasaq Adewale[1, *]

[1]Department of Chemistry, Lagos State University, Lagos, Nigeria

[2]Department of Chemistry, Lagos State University of Science and Technology, Lagos, Nigeria

Abstract

The release of unprocessed or moderately treated industrial wastewater, especially from the textile industry, poses significant environmental challenges due to the elevated levels of pollutants such as dyes. This research investigates the use of agricultural waste, specifically Raw Melon Husk (RMH), for the elimination of two different dyes which are Methylene Blue (MB) and Rhodamine 6G (R6G) utilizing the adsorption technique. RMH was characterized using Fourier Transform Infrared Spectroscopy and Scanning Emission Microscopy. Various experimental parameters were optimized, including pH, adsorbent dosage, initial dye concentration, contact time, and temperature. Optimal conditions for Methylene Blue (MB) and Rhodamine 6G (R6G) dyes removal were determined to be at pH 7 and 6, dosage of 1 g/L and 20 g/L, concentration of 30 mg/L and 50 mg/L, and a contact time of 30 minutes and 10 minutes respectively. The adsorption capacity and percentage removal for MB and R6G are 1.1084 mg/g and 94.5% as well as 1.345 mg/g and 94.20% respectively. The Temkin isotherm model best described the equilibrium data ($R^2 = 0.9966$) for MB while Langmuir model with $R^2 = 0.9857$ fitted best for R6G suggesting a monolayer biosorption capacity of 1.200 mg/g. The kinetics of both dyes followed a pseudo-second-order model with R^2 of 0.996 and 0.9998 respectively which inferred that the process is diffusion controlled. Thermodynamic studies indicated that the adsorption process for both dyes were exothermic and spontaneous. The melon husk has successfully been used for removing methylene blue and Rhodamine 6G from model wastewater. This study contributed to achieve SDG goals 3 and 6.

Keywords

Melon Husk (*Cucumeropsis manni),* Kinetics, Thermodynamics Bisorption, Rhodamine 6G Dye, Methylene Blue Dye

*Correspondence: Olowu Rasaq Adewale (Rasaq.olowu@lasu.edu.ng)

Received: 26 November 2025; **Accepted:** 24 February 2026; **Published:** 10 March 2026

1. Introduction

With the development and advancement in technology to satisfy human needs, comes harmful consequences and effects. These effects emerge in different forms of environmental pollution e.g. Water pollution [1]. A major technological advancement responsible for water pollution is from the textile industry [1]. Dyes are one of the most dangerous pollutants in water as far as environmental hazards are concern. During the manufacturing process of textiles, only a few of the dye stays on the fabric, the rest are discharged as waste into the water bodies [2]. This waste is very harmful to aquatic lives, human lives and the economy possibly causing disturbances in the food chain and diminishing biodiversity [3]. Hence, the removal of this dye from wastewater is prioritized as one of the most critical environmental problems to be solved [2-4].

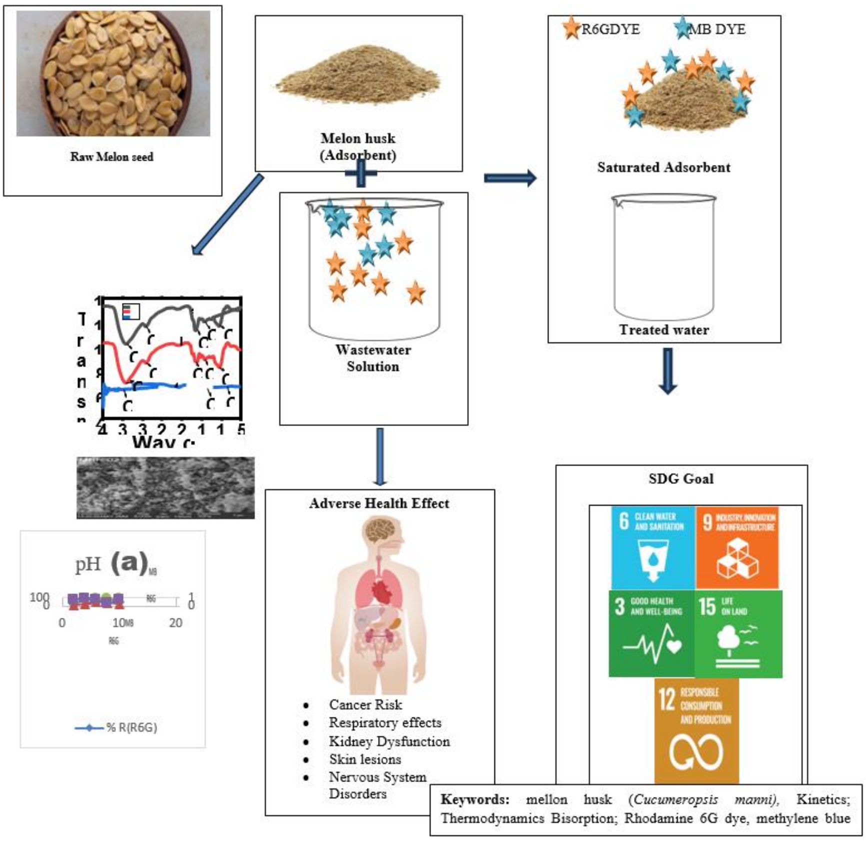

Figure 1. *Graphical Abstracts.*

Dye bearing effluents are treated in various ways. Sedimentation, chemical flocculation, coagulation, filtration and aeration are efficient traditional methods that are used in treating textile effluents [4]. However, there are several cons associated with this method. Such as, high energy consumption, offensive smell, toxic by-products, and huge capital cost [5]. In the last few years, to cover this gap, researchers needed to look for more efficient methods to improve the quality of textile wastewater effluent before discharging into the environment [5].

A relatively new approach discovered is known as biosorption. Biosorption can be defined as the separation of organic and inorganic material, including metals and dyes using live cells or parts of their biomass, such as bacteria, fungi, seaweed, various sludge materials, or byproducts of the fermentation industries [6]. The utilization of agricultural waste as adsorbents is very important for the removal of many pollutants from wastewater [5]. The biosorption behavior of agricultural products is defined as the ability of a surface to adsorb dye by utilizing agriculturally based materials [6].

This method is widely implemented for removing dye from wastewater because the process has high effectiveness compared to other techniques with various constraints [5]. The adsorption approach using agricultural waste is considered more efficient due to the high efficiency of removing dyes and no toxic by-products [2-5].

Considering that agricultural wastes have little to no commercial and economic value, coupled with the constraints of proper disposal. Hence, it is important to find efficient ways to utilize them [6]. Such materials are easily and locally available in developing and under-developed countries [5, 6]. From a socio-economic perspective, agricultural waste is inexpensive, and when waste is converted into an effective adsorbing reagent, agricultural waste expenditures are eliminated, and the adsorbing agent offers opportunities for commercialization [6].

Besides agricultural waste, other types of adsorbents like metal-organic frameworks (MOFs), metal materials, organic polymers, organic polymers have been utilized for dye adsorption (5-6, 18-21). These adsorbents generally have advantages like abundant surface areas and ample functional groups favoring the adsorption of dye molecules and other pollutants to them and leading to high adsorption efficiencies [7, 21-23].

In the present study, it aimed at the evaluation of the efficacy of raw melon husk (RMH) as a low-cost adsorbent for the removal of Methylene Blue (MB) and Rhodamine 6G (R6G) dyes from aqueous solutions. Comparing the adsorption capacities, optimal conditions, kinetics, equilibrium, and thermodynamic parameters to determine its potential as an efficient industrial waste treatment solution.

2. Materials and Methods

2.1. Preparation of Stock Solution

A stock solution of 1000 mg/L of dyes was prepared. The dye solutions were prepared by dissolving 1 g of Methylene Blue ($C_{16}H_{18}N3SCl$) and Rhodamine 6G ($C_{28}H_{31}ClN_2O_3$) in a 1000 mL volumetric flask and diluted up to the mark by addition of distilled water. Then the working solution was prepared from the stock to get desired experimental concentrations. The wavelength of absorbance of the adsorbate was determined using Perkin Elmer Lambda 356 UV-Vis spectrophotometer.

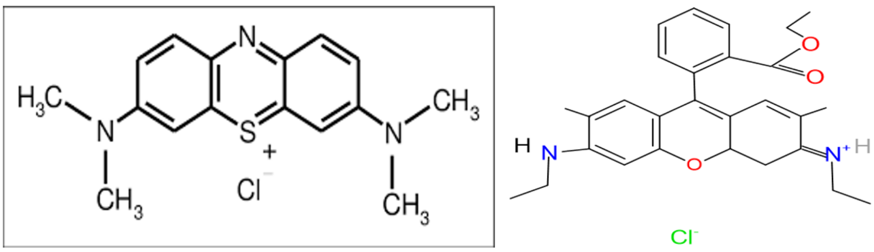

(a) (b)

Figure 2. (a) Structure of Methylene Blue (b) Structure of Rhodamine 6g.

2.2. Collection and Preparation of Adsorbent

The chosen precursor material, Raw Melon husk (RMH) which was used as a biosorbent in this study, was obtained from a local market, Iya-Iba market, Ojo, Lagos. Before use the melon husk was washed with tap water first, then distilled water conspicuously to remove dirt, dust and several surface impurities. The dried samples were ground in a blender and sieved to obtain a particle of desired size and stored in Plastic containers to use for adsorption experiments.

2.3. Batch Adsorption Experiment

The pH variation: The effect of pH on the equilibrium adsorption of Methylene Blue and Rhodamine 6G by RMH was investigated over a range of pH (2, 4, 6, 8 and 10) values at an initial concentration of 50 mg/L, using 50 mL of MB and R6G and 0.5 g of the adsorbents. The suspension was agitated using an orbital shaker (Model SSMI, SSL1-CCL) at a speed of 250 rpm for 120 minutes at 25 ℃, left to settle, and then filtered. Changes in pH of MB and R6G solution was accomplished by using 0.1 M HCl or 0.1 M NaOH to attain pH changes for the MB and R6G.

Dosage variation: The dosage variation experiment was achieved by using, 50 mL of the MB and R6G solution respectively varying dosage of the adsorbent (0.1 g, 0.3 g, 0.5 g, 0.7 g, 0.9 g, 1.0 g and 1.5 g) at pH 7 and 6 respectively. This experiment was conducted as described in the pH variation.

The concentration variation: This was done by using 50 mL of the MB and R6G solution with varying concentration (10, 30, 50, 70, 90 and 100 mg/L) at an optimal pH 7 and 6; 1.0 g of the adsorbent respectively.

Time variation: Time variation was performed by measuring 50 mL of 30 mg/L and 50 mg/L of MB and R6G solution respectively at pH 7 and pH 6 respectively with 0.25 g and 1.0 g of the melon husk adsorbent was used. The suspension was agitated using an orbital shaker at a speed of 250 rpm at time intervals (10, 30, 60, 90, 120 and 140 minutes). After shaking, the suspension is left to settle and was filtered.

Temperature variation: The optimal temperature process was achieved using 50 mL of 30 mg/L MB solution with 0.25 g of melon husk adsorbent and 50 mL of 50 mg/L R6G solution at pH 6 with 1.0 g of melon husk adsorbent. The suspension was agitated using an orbital shaker for an optimal time of 30 min and 10 min respectively at varying temperatures (25, 30, 35, and 40 ℃). All of the experiments were duplicated to check the reproducibility of data and the averages of the results were used for data analysis. The absorbance of the filtrate was determined using a SM 7504 UV-Vis spectrophotometer at 664 nm and 527 nm for MB and R6G respectively.

Data Treatment

Calculation of the removal of dye by melon husk adsorbent

The adsorption capacities were determined according to the following equation:

$$qe = \frac{(C_0 - C_e)V}{M} \quad (1)$$

Where; C_0 and C_e are the initial and final sorbate concentration in solutions, qe, V and M are the amount of sorbate sorbed (mg/g), volume of the solution (mL) and mass (g) of RMH sample, respectively.

C_o (mg L^{-1}) is the initial concentration of R6G and MB solution; C_e (mg L^{-1}) is the equilibrium concentration of R6G and MB in aqueous solution; V (L) is the volume of solution; m (g) is the mass of the biosorbent and q_e (mg g^{-1}) is the calculated R6G and MB biosorption amount onto the melon husk respectively.

Calculation of the percentage of dye removed by the adsorbent (RMH).

The percentage removal of dye was calculated using the following equation;

$$\% \ R = \frac{(C_0 - C_e)}{C_0} x \ \ 100 \quad (2)$$

Where; R is the removal efficiency of the metal ions adsorbent studied; C_0 is the initial metal ions concentration in solution (mg/L); C_e is the metal ions concentration removed by adsorbent at equilibrium (mg/L). [16-20].

2.4. Adsorption Isotherm

An adsorption isotherm helps to predict the applicability of an adsorption process using some physiochemical properties. Sorption isotherms were characterized by some constants which values express the surface properties and affinity of the sorbent and can also use to find the adsorptive capacity of a mass [20]. Different isotherm models were available, and three of them are selected in this study: Langmuir, Freundlich and Temkin models due to their simplicity and reliability.

2.4.1. Langmuir Isotherm

Langmuir theory assumes that adsorption was a kind of chemical process and that the adsorbed layer was unimolecular, that is, The Langmuir model assumes that the sorbent surface contains only one type of binding site so the energy of sorption is constant. The Langmuir isotherm model has the following form [21];

The Langmuir model in linear form;

$$\frac{C_e}{q_e} = \frac{C_e}{q_m} + \frac{1}{bq_m} \quad (3)$$

where q_e (mg g^{-1}) is the amount of the dye sorbed per unit mass of sorbent, C_e (mg g^{-1}) is the equilibrium dye concentration in the solution, q_m (mg g^{-1}) is the Langmuir constant related the maximum monolayer sorption capacity and b (L mg g^{-1}) is the constant related to the free energy or net enthalpy of adsorption.

The essential characteristics of Langmuir isotherm can be described by means of 'R_L' a dimensionless constant referred to as separation factor or equilibrium parameter. R_L can be calculated using the following equations [22-27];

$$RL = \frac{1}{1 + bC_O} \quad (4)$$

where C_o (mg L^{-1}) is the initial concentration of sorbate and b (L mg^{-1}) is the Langmuir constant described above. The R_L parameter is considered as more reliable indicator of adsorption. [16, 18].

The graph of Ce/qe against qe was plotted.

2.4.2. Freundlich Isotherm

The Freundlich isotherm model assumes a heterogeneous sorption surface with sites that have different energies of sorption and provides no information on the monolayer adsorption capacity [22]. The Freundlich model has the linear form;

$$\ln qe = 1/n \ln Ce + \ln Kf \quad (5)$$

where qe (mg g^{-1}) is the amount of the dye sorbed per unit mass of sorbent, Ce (mg g^{-1}) is the equilibrium dye concentration in the solution, Kf is a constant related to sorption capacity (mg g^{-1}) and 1/n is an empirical parameter related to sorption intensity. The value of n varies with the heterogeneity of sorbent and gives an idea for the favorability of sorption process. Favorable sorption conditions, $0 < n < 10$ or $0 < 1/n < 1$ [17-22, 27].

A plot of ln qe versus ln Ce was done.

2.4.3. Temkin Isotherm

The Temkin isotherm contains factors that take into account the interaction between the adsorbent and the adsorbate. This model assumes that the heat of adsorption of all molecules decreases linearly by increasing coverage. This isotherm is given by the equation below;

$$qe = ß \ln Ce + ß \ln kt \quad (6)$$

$$ß = RT / Bt \quad (7)$$

ß represents the heat of adsorption; R is the universal [23].

2.5. Adsorption Kinetics Modeling

Kinetic models are utilized to study the rate of the adsorption process and the potential rate estimating step. Pseudo first and second order kinetics models were applied in order to model the adsorption process.

2.5.1. Pseudo First Order Model

The pseudo first order has the linear form;

$$\ln (qe - qt) = \ln qe - k1t \quad (8)$$

where qe (mg g^{-1}) is the amounts of the dye biosorbed on the biosorbate at equilibrium; qt (mg g^{-1}) is the amounts of the dye biosorbed on the biosorbate at any time t; k1 (min^{-1}) is the rate constant of the first order model.

A ln (qe−qt) versus t plot.

2.5.2. Pseudo- Second Order Model

The pseudo-second-order model assumes that the adsorption process occurs through chemisorption, which involves the formation of a chemical bond between the adsorbate and the adsorbent surface. The model has the linear form;

$$t/q_t = t/q_e + 1/k_2q^2_e \quad (9)$$

Where; k_2 (g mg^{-1} min^{-1}) is the rate constant of the second-order equation; [17-19].

q_e (mg g^{-1}) is the maximum biosorption capacity;

q_t (mg g^{-1}) is the amount of biosorption at time t (min).

2.6. Adsorption Thermodynamic

The thermodynamic parameters including Gibbs free energy change (ΔG°), enthalpy (ΔH°), and entropy change (ΔS°), have a significant role to determine the feasibility, spontaneity and heat change for the biosorption process.

These parameters can be calculated using the equation

$$\Delta Go = -RT \ln Kd \quad (10)$$

where R is the universal gas constant (8.314 J mol^{-1} K^{-1}); T is the temperature (K); and K_d is the distribution coefficient [24-30], The K_d value was calculated using the equation

$$K_d = C_e / q_e \quad (11)$$

where q_e and C_e are the equilibrium concentration of R6G on biosorbent (mg/g) and the concentration of R6G after adsorption (mg L⁾, respectively [26-33, 40].

The enthalpy (ΔH°), and entropy change (ΔS°) of adsorption were estimated from the equation;

$\Delta G^o = \Delta H^o - T\Delta S^o$ and it has a linear form of:

$$\ln Kd = \frac{\Delta S^0}{R} + \frac{\Delta H^0}{RT} \quad (12)$$

The thermodynamic parameters of ΔH° and ΔS ° were obtained from the slope and intercept of the plot between $\ln K_d$ versus 1/T, gas constant; T is the absolute temperature in Kelvin; Kt and ß are the isotherm constant and can be gotten from the plot of qe versus Ce [16-21].

3. Result and Discussion

3.1. Characterization

The physiochemical properties of Melon husk were characterized using Fourier Transform Infrared Spectroscopy (FTIR) and Scanning Electron Microscope (SEM). FTIR was used to identify the presence of functional groups on the adsorbent surface while SEM was used for morphology investigation of the adsorbent before and after adsorption.

3.2. Fourier Transform Infrared (FTIR) Spectroscopy of Raw Melon Husk

Raw melon husk (RMH) biosorbent was analyzed using a Nicolet™ iS50 FT-IR spectrophotometer to substantiate the possible interactions of dyes onto biosorbent and its consequence on the biosorption behavior. The FTIR spectra of the biomass (RMH) revealed numerous absorption bands between the wavelength ranges of 4000 - 500 cm^{-1} showing transmittance of the biosorbent. Fourier transform infrared (FTIR) spectra of the raw melon-husk adsorbent and after adsorption of methylene blue (MB) and Rhodamine-6G (R6G) are shown in Figure 3. The spectrum of the raw melon husk displays the characteristic bands of lignocellulosic biomass: a broad O-H stretching band centered in the 3200-3600 cm^{-1} region (indicative of hydrogen-bonded hydroxyl groups from cellulose, hemicellulose and absorbed water), C-H stretching bands near 2850-2930 cm^{-1} (aliphatic $-CH_2$/$-CH_3$), a C=O/carbonyl/ester band in the region 1700-1730 cm^{-1} (associated with hemicellulose and lignin carbonyls), aromatic C=C and conjugated carbonyl vibrations around 1500-1600 cm^{-1}, and multiple C-O / C-O-C stretching bands between 1000 and 1250 cm^{-1} arising from cellulose/ether linkages. After adsorption of R6G (red spectrum) and MB (blue spectrum), significant spectral changes occur constantly with dye uptake and surface interaction which in agreement with earlier report [19-21, 26-28, 41]. Key observations are: O-H band changes. The broad O-H band becomes less intense and, in some cases, slightly shifted after dye adsorption, indicating involvement of surface hydroxyls in hydrogen bonding with dye molecules and partial displacement of physisorbed water. Carbonyl / aromatic region (≈1500-1730 cm^{-1}). The intensity and/or position of the C=O / aromatic bands change after adsorption, with the R6G spectrum showing larger modifications in the aromatic/C=O region than MB. This suggests stronger π-π interactions and/or electrostatic/coordination interactions between the xanthene/aromatic moieties of R6G and melon-husk aromatic/carbonyl groups. After adsorption, features attributable to aromatic ring vibrations and N-containing groups from MB and R6G appear or increase in intensity (notably in the 1400-1600 cm^{-1} and 1000-1150 cm^{-1} regions). These confirm the presence of both cationic dyes on the melon-husk surface [30, 41].

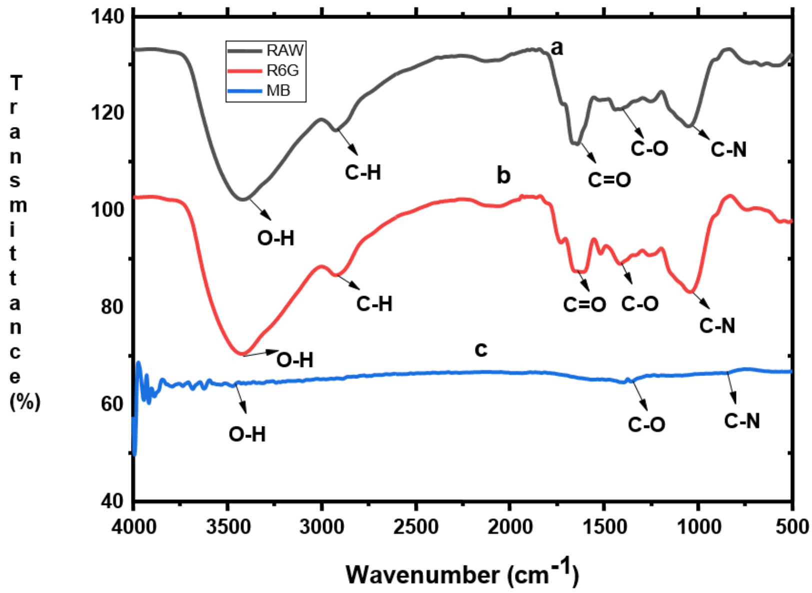

Figure 3. FTIR spectrum of (a) Melon Husk before adsorption and (b) after adsorption of R6G (c) after adsorption of MB.

3.3. Scanning Electron Microscope Sem and Edx Analysis

Scanning Electron Microscopy (SEM) and energy dispersive spectroscopy X-ray (EDX) (aTecnai G2F2OX-TTwin-MAT model) techniques was used to examine the surface morphology and determine the chemical makeup of the biomass surface respectively. The highly magnified view reveals a porous, granular structure with a range of particle sizes which can facilitates the adsorption process due to its surface reaction nature. In addition, these features are indicative of a high surface area, which is beneficial for adsorption and can enhance adsorption processes. The texture appears rough and irregular, suggesting a complex surface that can provide numerous adsorption sites for dye molecules of methylene blue and Rhodamine 6G. The presence of pores is evident from Figure 4a-b, which illustrates a homogeneously distributed network of small filamentous and fistulous crystallites. The matrix also exhibits luminous and non-luminous features, indicating the presence of metals dispersed throughout the organic matrix and on the surface as shown in Figure 5.

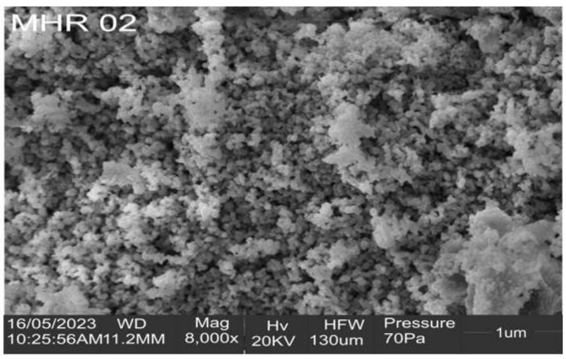

(a)

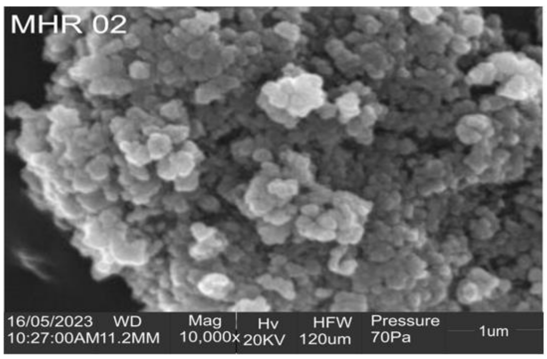

(b)

Figure 4. SEM morphology of melon husk before adsorption (a) at 8000x magnitude and (b) at 10000x magnitude.

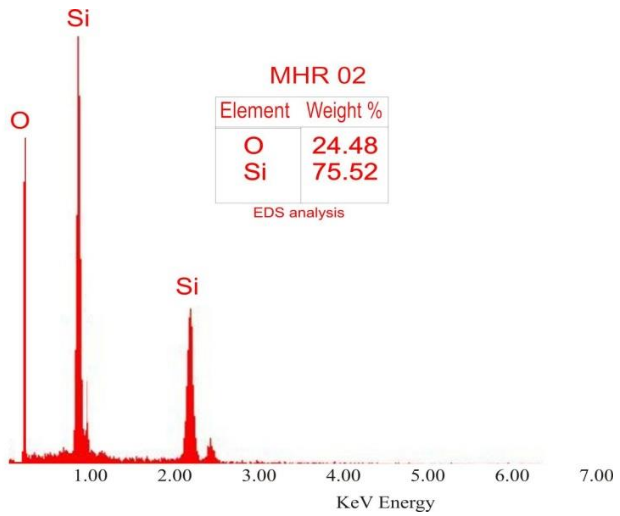

Figure 5. *Energy Dispersive Spectroscopy (EDS) analysis of melon husk before adsorption.*

3.4. Results and Discussion

3.4.1. Effect of Parameters on Adsorption Studie

(i). Effect of pH on Adsorption Studies

The pH of the solution has a strong influence on the adsorption of Rhodamine 6G (R6G) and Methylene Blue (MB) onto melon husk (Cucumeropsis manni), mainly because it affects both the surface charge of the adsorbent and the ionic form of the dye molecules. The variation in adsorption with pH is shown in Figure 6 (a_2), while the point of zero charge (pHpzc) of the melon husk surface is presented in Figure 6 (a_1). The pHpzc values were found to be around 6.0 and 7.0, indicating that the adsorbent surface is positively charged at lower pH values and becomes increasingly negatively charged as the pH rises. At acidic pH levels (pH 2-4), adsorption of both dyes was relatively low. This behavior can be explained by the protonation of surface functional groups such as -OH and -COOH, which gives the adsorbent a positive surface charge. As a result, electrostatic repulsion occurs between the adsorbent and the cationic dye molecules, while excess hydrogen ions compete with the dyes for available adsorption sites. Together, these effects limit dye uptake at low pH. As the pH increased toward the pHpzc region, adsorption improved significantly and reached a maximum at pH 6 for both dyes. The removal of R6G increased from 28.6% at pH 2 to 88.93% at pH 6, while MB removal increased from 80.75% to 92.01% over the same pH range. This enhancement is mainly due to reduced surface protonation and weaker electrostatic repulsion, which allow stronger dye-adsorbent interactions such as electrostatic attraction, hydrogen bonding, and π-π interactions to occur. When the pH was increased beyond 6, a gradual decrease in adsorption was observed for both R6G and MB. Although the adsorbent surface becomes negatively charged above the pHpzc, the reduction in adsorption may be linked to weaker effective electrostatic interactions, increased dye solubility, and competition from hydroxyl ions for active sites. Excess negative surface charge at higher pH may also hinder efficient dye attachment. Overall, the adsorption behavior of R6G and MB on melon husk is largely controlled by the surface charge properties of the adsorbent, as confirmed by the pHpzc results. The close agreement between the optimum adsorption pH and the pHpzc region highlights the key role of electrostatic interactions and supports the suitability of Cucumeropsis manni husk as a low-cost biosorbent for cationic dye removal under mildly acidic to near-neutral conditions, in line with previous reports on lignocellulosic agricultural wastes [26-33].

(ii). Effect of Adsorbent Dosage on Adsorption Studies

The effect of adsorbent dosage on the adsorption of MB and R6G was considered at a constant initial metal ion concentration of 2.053. mg/g and 3.005 mg/g respectively. As the dosage of melon husk increases from 0.1 g to 1.0 g, the amount of MB adsorbed decreases from 2.05 mg/g to 0.1688 mg/g as the dosage increases due to the greater surface area and more adsorption sites, although the adsorption capacity decreases with higher dosage as shown in Figure 6b. This behavior is attributed to the equilibrium reached between surface dye concentration and the MB dye solution at higher dosages. Similarly, the amount of R6G adsorbed decreases from 3.005 mg/g to 0.398 mg/g, while the% removal increases from 58.18% to 79.04%, indicating an optimal dosage of 1.0 g (Figure 5b).

(iii). Effect of Initial Metal Ion Concentration on Adsorption Studies

As the initial concentration of MB increases from 10 mg/L to 100 mg/L, the amount of MB uptake on melon husk increases from 0.58 mg/g to 0.78 mg/g, but a decrease in percent adsorption from 94.13% to 87.95%, due to the enhanced interaction between dye molecules and the adsorbent surface. Similarly, for R6G an increase in initial concentration from 10 mg/L to 100 mg/L leads to an increase in adsorption capacity from 0.26 mg/g to 2.40 mg/g, with a corresponding increase in percentage removal from 84.04% to 95.07% [18-21, 28, 32-38]. The higher percentage adsorption at lower initial concentrations for both dyes is attributed to the high ratio of adsorptive surface to dye concentration, which means fewer dye molecules compete for available binding sites on the adsorbent [28, 30], whereas with increasing dye concentration, this ratio decreases, leading to reduced percent adsorption. Similar observations have been reported by others [29, 30], where a decrease in percent adsorption with increasing initial concentration of adsorbate resulted in increased adsorption capacity.

(iv). Effect of Contact Time on Adsorption

The effect of contact time on the adsorption of MB and R6G dyes on melon husk was examined at constant optimal dye concentration of 30 mg/L and 50 mg/L respectively. The result of the adsorption shown in Figure 6d revealed an initial rapid uptake of MB dye achieving over 89% adsorption within the first 10 minutes, followed by a slower increase up to approximately 120 minutes to 96.2%, which was identified as the equilibrium time. In contrast, R6G, exhibited a similarly rapid initial phase, with adsorption percentages climbing from 94.2% to a peak of 96.49% over 10 minutes, corresponding to a gradual increase in adsorbed amount from 1.345 mg/g to 1.380 mg/g. This pattern suggests that both dyes benefit from an abundance of available binding sites during the early stages of adsorption, facilitating their rapid uptake onto melon husk surfaces.

(v). Effect of Temperature on Adsorption Studies

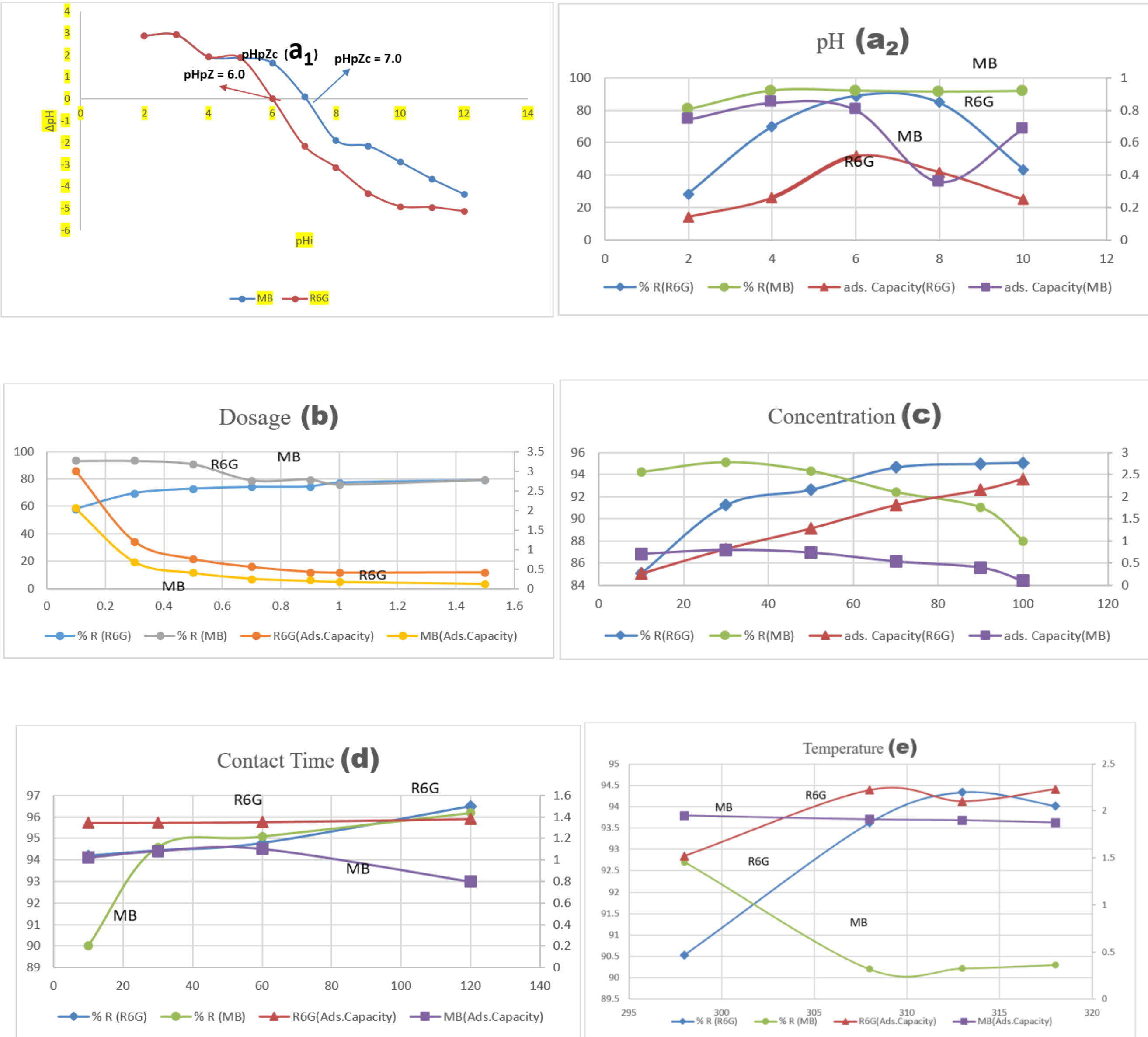

Figure 6*. Effect of (a*1*) point of Zero charge, (a*2*) pH (b) adsorbent dose (c) dye concentration, (d) contact time and (e) Temperature on biosorption of R6G and MB dyes.*

In comparing the adsorption behaviors of MB and R6G dyes on melon husk, the effect of temperature on the adsorption process was studied at distinct temperature from 298K to 318K as shown in Figure 6e. Notably, the adsorption of MB onto RMH exhibits a reduction in adsorption capacity, decreasing from 1.96 mg/g (92% removal) to 1.88 mg/g (90% removal) as the temperature rises from 298 K to 318 K, indicating an exothermic nature of the MB adsorption process under these conditions and a low energy requirement for the MB adsorption onto the melon husk. This decrease could be credited to a decrease in mobility due to a decrease in the number of active surface sites for adsorption by melon husk at higher temperatures thus decreasing the number of MB that interact with active sites of the biosorbent. Conversely, for R6G, the percentage removal increases from 90.53%

at 298 K to 94.01% at 318 K, accompanied by a corresponding rise in uptake from 1.52 mg/g to 2.23 mg/g. This highlights the robust biosorption capability of melon husk for R6G across different temperatures, as illustrated in Figure 6d.

3.4.2. Adsorption Isotherms Studies

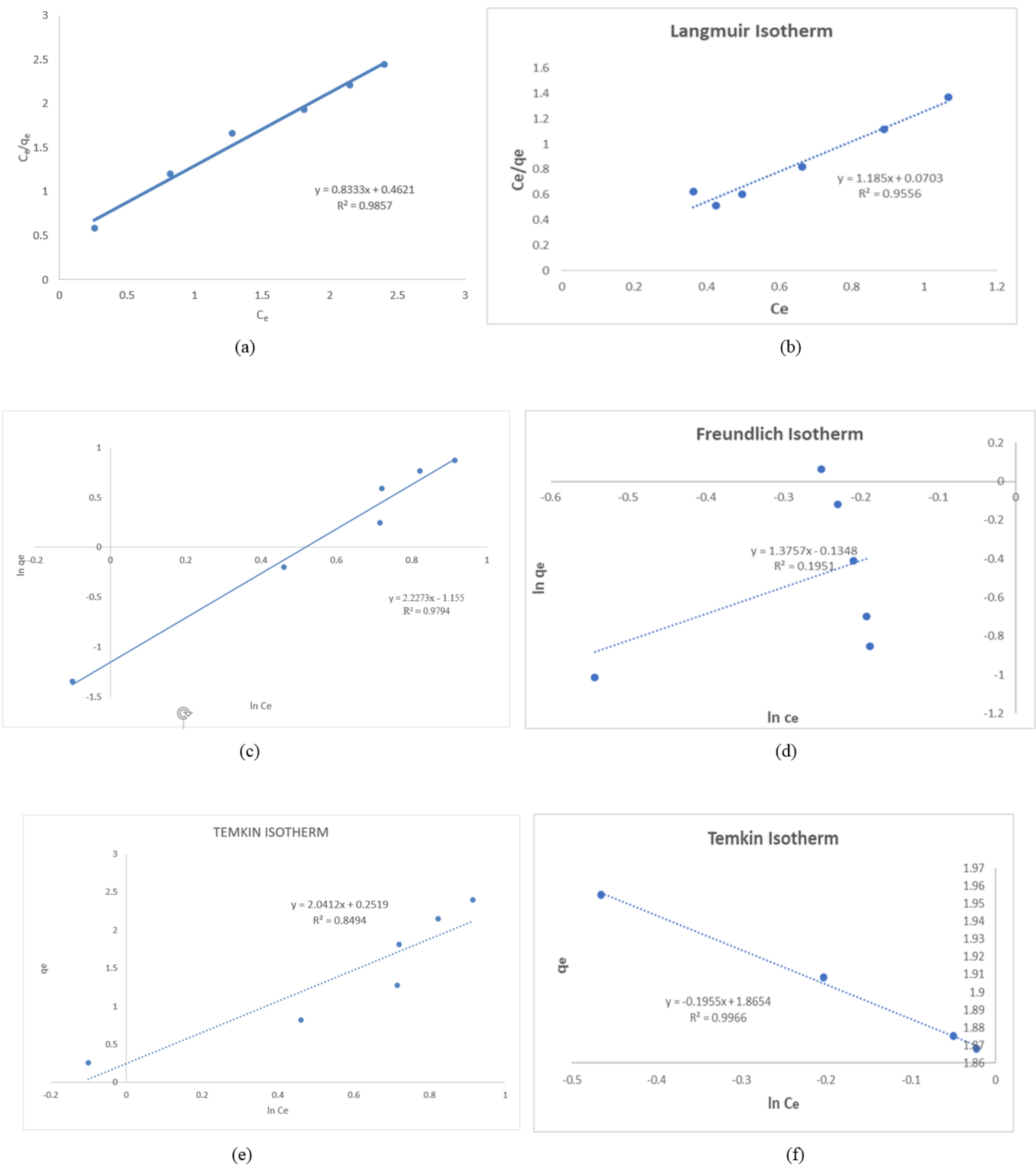

Figure 7*. Adsorption isotherm plot (a, b,) Langmuir for R6G and MB, (c, d) Freundlich for R6G and MB) (e, f) Temkin for for R6G and MB onto melon husk.*

This work examined the adsorption of methylene blue dye and Rhodamine 6G (R6G) onto melon husk using the Langmuir, Freundlich, and Temkin isotherm models. The results of the study, as presented in Table 1, indicate that the Langmuir and Temkin models provide a good fit for the data, with R^2 values ranging from 0.9957 to 0.9966 as shown in Figures 7a-f. The correlation coefficient values indicated that the Langmuir model is a better fit for R6G which may be due to both homogeneous active sites on the surface of the melon husk which in agreement with earlier report [30, 33-37] while the

Temkin model is more suitable for MB as shown in Table 1. The maximum adsorption capacity, q_m, was calculated from the Langmuir plots for each dyes. The analysis showed that melon husk posses a higher adsorption capacity for R6G compared to MB. The approach to zero of the R_L with increase in the Co value, indicated that the melon husk is a suitable biosorbent for the biosorption of R6G from aqueous solutions. The Temkin isotherm model was found to be suitable for the adsorption of MB onto melon husk. The values of K_t were determined from the intercept and slope of the graph for each dye respectively and are as well presented in Table 1. The results indicate that R6G has the strongest adsorption tendency towards melon husk followed by MB. Additionally, the n values obtained for the dyes adsorption onto melon husk are less than unity, suggesting that the adsorption process is chemical in nature.

Table 1. *Adsorption isotherm parameters for the adsorption of Rhodamine 6G and Methylene Blue onto melon husk (Cucumeropsis manni).*

Isotherm Models	R6G	MB
Langmuir		
C_o (mg/L)	50	30
Q_{max} (mg/g)	1.200	0.843
Q_e (mg/g)	1.280	0.426
b (L/g)	1.803	16.95
R_L	0.011	0.007
R^2	0.9857	0.9556
Freundlich		
1/n	2.227	1.376
K_F	0.315	0.874
R^2	0.9794	0.1951
Temkin		
K_t (L/mg)	1.133	0.8494
R^2	0.210	0.9966

3.4.3. Adsorption Kinetic Studies

To examine the impact of time on the adsorption process and determine the service time of the adsorbent, the adsorption kinetic of the dyes using the prepared adsorbents was assessed. Elovich's pseudo-first and pseudo-second-order models were applied to analyze the experimental data and identify potential mechanisms involved in adsorption [26-30, 39, 40]. The adsorption kinetics are illustrated in Figure 8a-d and the model fitting parameters are summarized in Table 2. The results suggest that the experimental data was better fitted by the pseudo-second-order reaction than by the pseudo-first-order reaction as shown by the correlation coefficient, R^2 values of 0.9996 and 0.9998, obtained which are close to unity which indicated that the dyes exhibited diffusion controlled on the surface of the melon husk (26, 40).

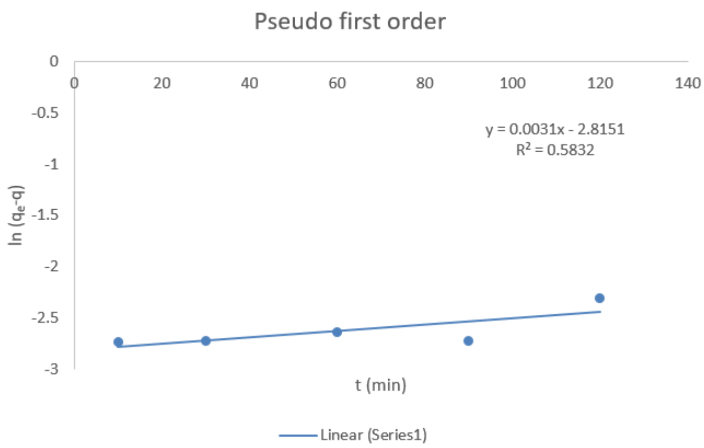

(a)

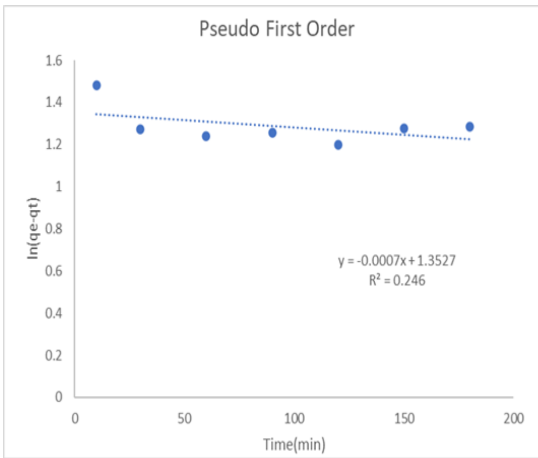

(b)

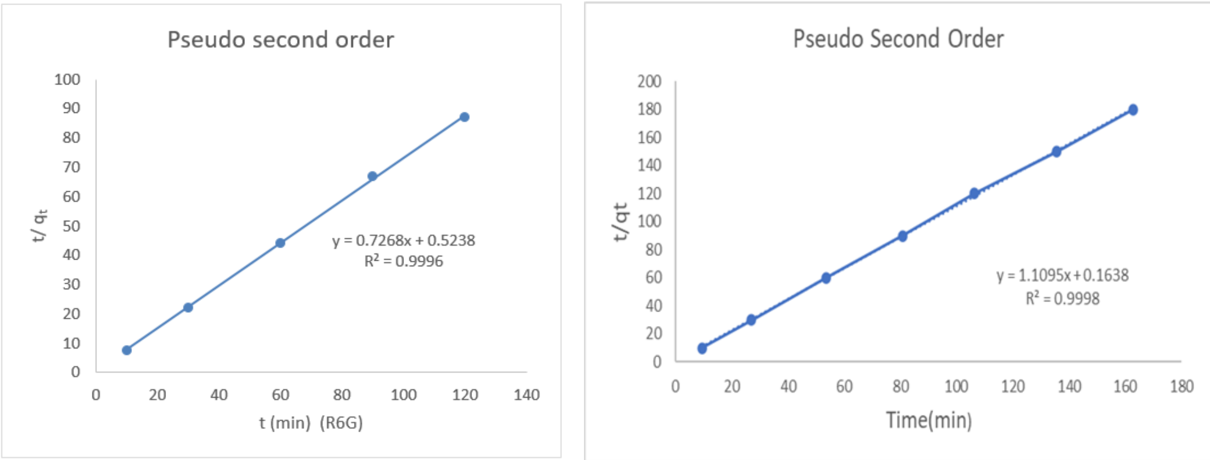

(c) (d)

Figure 8. *Pseudo first order plot (a) for R6G and (b) for MB and Pseudo second order plot (c) for R6G and (d) for MB onto melon husk (Cucumeropsis manni).*

Table 2. *Parameters for various kinetic models of Rhodamine 6G and Methylene Blue using Cucumeropsis manni.*

Kinetic Models	**R6G**	**MB**
Pseudo-first order		
C_O (mg/l)	50	30
Qe (mg/g)	0.0599	3.8679
K_1 (min^{-1})	1.002	0.0007
R^2	0.5832	0.2460
Pseudo-second order		
C_O (mg/l)	50	30
Qe (mg/g)	1.380	0.9013
K_2	06296	7.513
R^2	0.996	0.9998

Thermodynamic investigation on Adsorption

The standard enthalpy ΔH° and entropy ΔS° were calculated using the slope and intercept of the graph of ln K against T^{-1}, as depicted in Figure 9 a, b and Table 3. A negative value was obtained for ΔG° across all temperatures (25°C-40°C) examined. For both R6G and MB, the negative value of ΔGº increased from −1.91 to −0.65 kJ mol^{-1} and an increase from -2.81 to -1.79 kJ mol^{-1} with an increase in temperature respectively indicating the spontaneous nature of biosorption of both dyes. The negative values of ΔHº (-22.88 kJ mol^{-1} & -13.41 kJ mol^{-1}) and ΔSº (-70.92 J mol^{-1} K^{-1} & -36.87 J mol^{-1} K^{-1}) which depicts the thermodynamic analysis demonstrated the exothermic nature of biosorption with decreasing randomness at the solid/solution interface during the biosorption of R6G and MB onto melon husk.

Table 3. *Thermodynamic Parameter of adsorption.*

Temp (°K)	**ΔG (kJ $mole^{-1}$)**		**ΔH (kJ $mole^{-1}$)**		**ΔS (J K^{-1} $mole^{-1}$)**	
	R6G	**MB**	**R6G**	**MB**	**R6G**	**MB**
298	-1.91	-2.81	-22.88	-13.41	-70.92	-36.87
308	-0.81	-1.63				
313	-0.41	-2.17				
318	-0.65	-1.79				

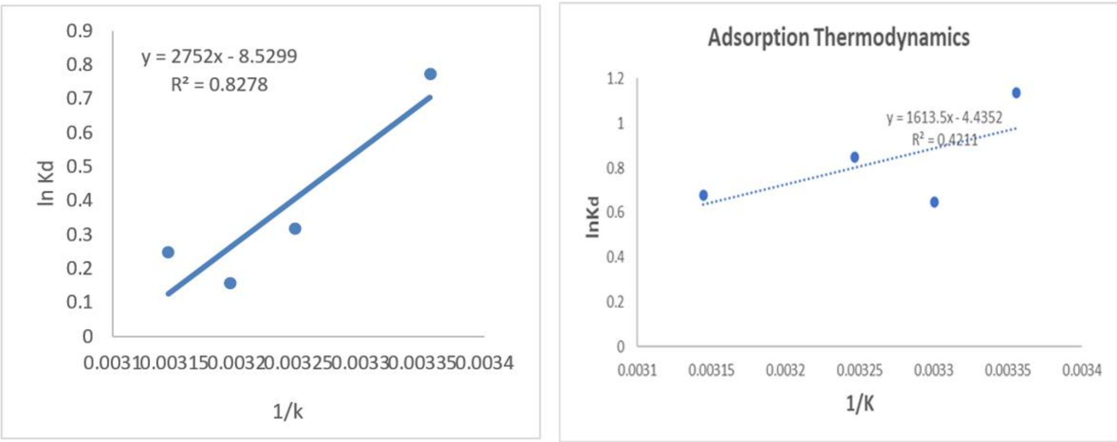

(a) (b)

Figure 9. Plot of Van't Hoff for adsorption of (a) R6G (b) MB) onto Melon husk.

4. Conclusion

Comparative Analysis of MB and R6G Dye Removal Using Melon Husk as an Adsorbent Raw melon husk (RMH) has demonstrated effectiveness as a low-cost adsorbent for the removal of both Rhodamine 6G (R6G) and Methylene Blue (MB) dyes from aqueous solutions. The biosorbent demonstrated an increased ability to remove these dyes at both acidic and neutral pH, with the optimal removal at a slightly acidic pH of 6 for R6G and pH 7 for MB. The optimal conditions for other parameter for R6G adsorption indicated adsorbent dosage of 20 mg/L, initial concentration of 50 mg/L, and an equilibrium time of 120 minutes while for MB the adsorbent dosage of 1 g/L, initial concentration of 30 mg/L, and an equilibrium time of 30 minutes were established. The pseudo-second-order kinetic model was a better fit for the adsorption of both dyes than the pseudo-first-order model, with a higher correlation coefficient. Thermodynamic studies showed that the adsorption process was exothermic and spontaneous, with a negative Gibbs free energy of adsorption. The isotherm and thermodynamic data indicated that the adsorption mechanism was generally physisorption due to low energy. This research work supports the UN Sustainable Development Goals by enhancing efficient wastewater treatment and safeguarding human health through the removal of textiles dyes from wastewater.

Abbreviations

FTIR	Fourier-transform Infrared Spectroscopy
pH	Potential of Hydrogen
qe	Adsorption Capacity at Equilibrium (mg/g)
R2	Coefficient of Determination
SEM	Scanning Electron Microscopy
WHO	World Health Organization
°C	Degrees Celsius
MB	Methylene Blue
R6G	Rhodamine 6G
RMH	Raw Melon Husk
XRD	Xray Difraction

Author Contributions

Onwordi Chionyedua Theresa: Conceptualization, Data curation, methodology, supervision, Writing – review & editing

Adetunji Ibrahim Olaniyi: Data curation, Methodology resources, Writing – original draft

Borokinni Ridwan Aderenle: Data curation, Methodology resources, Writing – original draft

Oyewole Toyib Seun: Supervision, software, Project administration, validation, visualization

Uche Cosmos Chinedu: Methodology, resources, software

Osifeko Olawale Lawrence: Supervision, software, Project administration

Tovide Oluwakemi Omotunde: Data curation, Methodology, resources, validation

Osundiya Medinat Olubunmi: Data curation, Methodology, resources, validation

Dodo Salimah Wuraola: Supervision, software, Project administration, validation

Akoro Seide Modupe: Methodology, resources, investigation, software

Olowu Rasaq Adewale: Conceptualization, Data curation, methodology, supervision, validation, visualization, Writing – review & editing

Data Availability Statement

The data is available from the corresponding author upon reasonable request.

Conflicts of Interest

The authors declare no conflicts of interest.

References

[1] Rahmiana Zein, Jofi Satrio Purnomo, Putri Ramadhani, Safni, Matlal Fajri Alif, Chessia Nodifa Putri, Enhancing sorption capacity of methylene blue dye using solid waste of lemongrass biosorbent by modification method, Arabian Journal of Chemistry, Volume 16, Issue 2, 2023, 104480.

[2] Arushi Garg, Lalita Chopra, Dye Waste: A significant environmental hazard, Materials Today: Proceedings, Volume 48, Part 5, 2022, Pages 1310-1315, ISSN 2214-7853, https://doi.org/10.1016/j.matpr.2021.09.003

[3] Oyewole T S, Olowu R. A, Osundiya M. O, Tovide O. O, Akanbi P. J, Abosede S. O, Ejire A. A (2025). Photocatalytic degradation studies of Indigo Carmine dye by Green-Synthesized silver nanoparticles from theobroma Cacao extracts. J Phys Chem Biophys. 15: 1-9.

[4] Rania Al-Tohamy, Sameh S. Ali, Fanghua Li, Kamal M. Okasha, Yehia A.-G. Mahmoud, Tamer Elsamahy, Haixin Jiao, Yinyi Fu, Jianzhong Sun a (2022). A critical review on the treatment of dye-containing wastewater: Ecotoxicological and health concerns of textile dyes and possible remediation approaches for environmental safety Ecotoxicology and Environmental Safety 231 page 113160.

[5] Adel Ali Al-Gheethi, Qasdina Marsya Azhar, Ponnusamy Senthil Kumar, Abdiadim Abdirizak Yusuf, Abdullah Khaled Al-Buriahi, Radin Maya Saphira Radin Mohamed, Muhanna Mohammed Al-shaibani (2022)., Sustainable approaches for removing Rhodamine B dye using agricultural waste adsorbents: A review, Chemosphere, Volume 287, Part 2, 132080.

[6] Muhammed Safa Çelik, Şenay Akkuş Çetinus, Ali Fazıl Yenidünya, Serap Çetinkaya, Burak Tüzün,(2023). Biosorption of Rhodamine B dye from aqueous solution by Rhus coriaria L. plant: Equilibrium, kinetic, thermodynamic and DFT calculations, Journal of Molecular Structure, Volume 1272, 134158.

[7] Sah, M. K., Edbey, K., EL-Hashani, A., Almshety, S., Mauro, L., Alomar, T. S., AlMasoud, N., & Bhattarai, A. (2022). Exploring the Biosorption of Methylene Blue Dye onto Agricultural Products: A Critical Review. Separations, 9(9), 256.

[8] Yawei Shi, Qian Chang, Tongwen Zhang and Guobin Song (2022). A Review on Selective Dye Adsorption by Different Mechanisms. Journal of Environmental Chemical Engineering 10(6): 108639.

[9] Maheshwari, K., Agrawal, M., and Gupta, A. B. (2021), "Dye pollution in water and wastewater". Novel Materials for Dye-containing Wastewater Treatment, 1-25.

[10] Li, W., Mu, B., and Yang, Y. (2019), "Feasibility of industrial-scale treatment of dye wastewater via bio-adsorption technology," Bioresource technology, 277, 157-170.

[11] Nasseh, N., Arghavan, F. S., Rodriguez-Couto, S., and Hossein Panahi, A. (2022), "Synthesis of $FeNi_3/SiO_2/CuS$ magnetic nano-composite as a novel adsorbent for Congo Red dye removal," International Journal of Environmental Analytical Chemistry, 102, 2342-2362.

[12] Li, F., Katz, L. and Hu, Z. (2019). Adsorption of major nitrogen-containing components in microalgal bio-oil by activated carbon: equilibrium, kinetics, and ideal adsorbed solution theory (IAST) model. ACS Sustainable Chemistry & Engineering*, 7(19), 16529-16538*.

[13] Olowu R. A, Osundiya M. O, Sobola A. O, Osifeko O. L, Tovide O. O, Oyewole T. S, Elesho A. O,, Onifade O. O,, Majolagbe A. O, Onwordi C. T, and 1 Adejare A. A (2024). Kinetics, thermodynamic and isotherms modeling of the equilibrium sorption of Pb (II), Ni (II), And Cd (II) ions into tiger nut chaff (cyperus esculentus) from model wastewater. Physical Chemistry 13(12) 19-31.

[14] Han, R., Wang, Y., Han, P., Shi, J., Yang, J. and Lu, Y. (2006). Removal of methylene blue from aqueous solution by chaff in batch mode, Journal of Hazardous Material. 137(1), 550-557.

[15] G. Annadurai, S. R. Juang and J. D. Lee, (2002). Use of Cellulose-Based Wastes for Adsorption of Dyes from Aqueous Solutions," Journal of Hazardous Materials, Vol. 92, No. 3, pp. 263-274.

[16] Osundiya M. O, Olowu R. A, Onifade O. O, Elesho A O, Osifeko O. L, Oyewole T. S, Tovide O. O, Balogun S. R, Adejare A. A, Anko S. O, Shotonwa I. O, Onwordi C. T (2024). Isotherms, Kinetics and Thermodynamic Investigation of the Adsorptive Capacity of Chrysophyllum Albidum Seed Shell an Agro-Waste for the Removal of Heavy Metals in Synthetic Wastewater. International Journal of Materials and Chemistry; 14(3): 37-48. https://doi.org/10.5923/j.ijmc.20241403.02

[17] R A Olowu, M A, Osundiya, T. S Oyewole, Onwordi C. T, Yusuf O K. Osifeko O. L Tovide O O (2022) Equilibrium and Kinetic Studies for the Removal of Zn (Ii) and Cr (Vi) Ions from Aqueous Solution Using Pineapple Peels as an Adsorbent. European Journal of Applied Sciences 10(5) 34-47.

[18] Himanshu Patel (2021). Comparison of batch and fixed bed column adsorption: a critical review. International journal of Environmental Science and Technology 19(2-3), https://doi.org/10.1007/s13762-021-03492-y

[19] María Dominguez, Jeamilette Mendoza, Katherine Figueroa (2024). Adsorption of methylene blue dye using common walnut shell (Juglans regia) like biosorbent: implications for wastewater treatment. Green Chemistry Letters and Reviews 17(1).

[20] Yasemin İşlek Coşkun (2023) Adsorptive methylene blue removal using modified agricultural wastes. Desalination and Water Treatment 315, 49-649-61 https://doi.org/10.5004/dwt.2023.30095

[21] Nisreen S. Ali, Talib M. Albayati, Issam K. Salih (2024). Studying the kinetics and removal mechanism of the methylene blue dye in a continuous adsorption process using prepared mesoporous materials. Water Practice and Technology 19(7): 2799-2815. https://doi.org/10.2166/wpt.2024.162

[22] Oyewole T. S, Inuikim E. A, Osundiya M. O, Osifeko O. L, Olowu RA, Isaac I. B, Adejare A. O, Oresanya A. A (2023).. Equilibrium, thermodynamics, kinetics of adsorption of CO_3^{2-} and SO_4^{2-} ions on modified plantain peels. Int J Eng Res Sci (IJOER).

[23] Medinat Oshundiya, Abdullahi Sobola, Toyib Oyewole, Oluwakemi Sarah, Sewanu K, Rasaq Olow (2024). Kinetics, isotherms, and thermodynamics studies of Pb^{2+} and Mn^{2+} adsorption from model wastewater solution using Raw Phoenix dactylifera L. seed. J Res Rev Sci. 11: 30-46.

[24] . Hasan, B. S.,, Duygu, O., and Celal, D. (2009). Biosorption of Rhodamine 6G from aqueous solutions onto almond shell (Prunus dulcis) as a low cost biosorbent. 252, 81-87.

[25] Gund, N. N., Marmat, B. M., Salunke, A. S., Sonar, J. P., Dokhe, S. A., Zine, A. M., Thore, S. N. and Pardeshi, S. D. (2021). Removal Of Rhodamine 6G From Aqueous Solution By Adsorption On Biosorbent Prepared From Hyptis Suaveolens (Vilayti Tulsi): Kinetic, Equilibrium And Thermodynamic Study. International Journal of Chemical and Physical Sciences. 10(2), 1-8.

[26] . Da Silva, A. M. B., Serrão, N. O., de Gusmão Celestino, G., Takeno, M. L., Antunes, N. T. B., Iglauer, S., … Maia, P. J. S. (2019). Removal of rhodamine 6G from synthetic effluents using Clitoria fairchildiana pods as low-cost biosorbent. Environmental Science and Pollution Research, 27(3), 2868-2880.

[27] Suwunwong, T., Patho, P., Choto, P., & Phoungthong, K. (2020). Enhancement the rhodamine 6G adsorption property on Fe_3O_4-composited biochar derived from rice husk. Materials Research Express, 7(2), 025511.

[28] El-Kammah M, Elkhatib E, Gouveia S, Cameselle C, Aboukila E.(2022). Enhanced removal of indigo carmine dye from textile effluent using green cost-efficient nanomaterial: Adsorption, kinetics, thermodynamics and mechanisms. Sustain Chem Pharm; 29: 100753.

[29] Adel M, Ahmed MA, Mohamed AA. (2021). Effective removal of indigo carmine dye from wastewaters by adsorption onto mesoporous magnesium ferrite nanoparticles. Environ Nanotechnol Monit Manag. 16: 100550.

[30] Eberlanny Moraes Rolim Andreza Miranda Barata da Silva · Joel dos Santos Batista Naiany Oliveira Serrão · Leticia Oliveira Laier · Flávio Augusto de Freitas · Gustavo Frigi Perotti · Dominique Fernandes de Moura do Carmo · Gustavo de Gusmão Celestino · Paulo José Sousa Maia (2024). Removal of rhodamine B and methylene blue using residual Onecarpus bacaba Mart fibers as biosorbent: kinetic and thermodynamic parameters. Discover Water 4(13) pg 1-18 | https://doi.org/10.1007/s43832-024-000580

[31] Elias, K. D., Ejidike, I. P., Mtunzi, F. M. & Pakade, V. E. (2021). Endocrine disruptors-(estrone and β-estradiol) removal from water by nutshell activated carbon: Kinetic, isotherms and thermodynamic studies. Chemical Thermodynamics and Thermal Analysis, 3-4, 100013.

[32] Hridoy Roy, Md. Shahinoor Islam, M. Tanvir Arifin, Shakhawat H. Firoz (2022). Chitosan-ZnO decorated Moringa oleifera seed biochar for sequestration of methylene blue: Isotherms, kinetics, and response surface analysis. Environmental Nanotechnology, Monitoring & Management 2022, 18, 100752. https://doi.org/10.1016/j.enmm.100752

[33] Y. Bulut, N. Gozubenli and H. Aydın, "Equilibrium and Kinetics Studies for Adsorption of Direct Blue 71 from Aqueous Solution by Wheat Shells," Journal of Hazardous Materials, Vol. 144, No. 1-2, 2007, pp. 300-306. https://doi.org/10.1016/j.jhazmat.2006.10.027

[34] Gallego-Ramírez C, Chica E, Rubio-Clemente A (2024). Elimination of indigo carmine in water by Pinus patula biochar: adsorption process optimization, kinetics and isotherms. J Environ Chem Eng 12: 112425. https://doi.org/10.1016/j.jece.2024.112425

[35] Ferreira RM, de Oliveira NM, Lima LLS et al (2019). Adsorption of indigo carmine on Pistia stratiotes dry biomass chemically modified. Environ Sci Pollut Res 26: 28614-28621.

[36] I. A. W. Tan, A. L. Ahmad and B. H. Hameed (2008), "Adsorption of Basic Dye Using Activated Carbon Prepared from Oil Palm Shell: Batch and Fixed Bed Studies," Desalination, Vol. 225, No. 1-3, pp. 13-28.

[37] C. Saniz-Diaz and A. Griffiths (2000), "Activated Carbon from Solid Wastes Using a Pilot Scale Batch Flaming Pyrolyser," Fuel, Vol. 79, No. 15, pp. 1863-1871.

[38] Annadurai, G., Juang, R.-S., & Lee, D.-J. (2001). Adsorption of rhodamine 6g from aqueous solutions on activated carbon. journal of environmental science and health, part a, 36(5), 715-725.

[39] Nethaji, S., Sivasamy, A., & Mandal, A. B. (2013). Adsorption of methylene blue onto activated carbon prepared from biomass material. Journal of Environmental Sciences, 25(5), 975-985.

[40] Bello, O. S., & Ahmad, M. A. (2012). Adsorption characteristics of Rhodamine B dye onto periwinkle shell-derived activated carbon. Journal of Chemistry, 2012, 1-12.

[41] M. Alkan, M. Doğan, Y. Turhan, Ö. Demirbaş, P. Turan (2008),. Adsorption kinetics and mechanism of maxilon blue 5G dye on sepiolite from aqueous solutions Chem. Eng. J., 139 pp. 213-223.

Research Field

Onwordi Chionyedua Theresa: Analytical/environmental chemistry

Adetunji Ibrahim Olaniyi: Analytical/environmental chemistry.

Borokinni Ridwan Aderenle: Analytical/environmental chemistry

Oyewole Toyib Seun: Physical Chemistry & Material Science

Osifeko Olawale Lawrence: Physical Chemistry & Material Science

Tovide Oluwakemi Omotunde: Nano/Environmental Chemistry

Osundiya Medinat Olubunmi: Surface/ Environmental Chemistry

Akoro Seide Modupe: Organic/Environmental Chemistry

Olowu Rasaq Adewale: Physical-Electroanalytical/ Environmental and Nano/material Science